Unsaturated Zone Hydrology for Scientists and Engineers

James A. Tindall, Ph.D.

United States Geological Survey, National Research Program
Department of Geography and Environmental Sciences, University of Colorado Denver

James R. Kunkel, Ph.D., P.E.

Knight Piésold, LLC, Denver, Colorado;
Department of Geology and Geological Engineering, Colorado School of Mines

with

Dean E. Anderson, Ph.D.

United States Geological Survey, National Research Program

PRENTICE HALL
Upper Saddle River, New Jersey 07458

11

Effects of Infiltration and Drainage on Soil-Water Redistribution

INTRODUCTION

Infiltration is the process by which water passes across the atmosphere–soil interface and enters a given soil column. The time-rate at which water (or another liquid) infiltrates the soil across the atmosphere–soil interface is known as the infiltration rate. The total volume of liquid crossing the interface is known as the cumulative infiltration. Quantitatively, infiltration rate is the volume of liquid entering the soil per unit area in a unit time.

This chapter defines terms and conditions essential to understanding the infiltration process during a water-input event, although infiltration of other liquids can be understood as an extension of the liquid characteristics presented in other chapters. This chapter also describes approaches to theoretical and practical calculation of infiltration and quantitatively discusses the variables that control the process. Some of the well-known and practical infiltration models are presented and discussed, along with examples of the infiltration process. Conditions affecting infiltration also change as a result of antecedent infiltration events; such processes are briefly discussed here. The reader is referred to chapter 13 for applied modeling of the redistribution process as a result of infiltration from a single event and antecedent events.

In engineering, infiltration capacity is often used and is defined as the maximum rate at which liquid can be moved into the soil in a given condition, and as such, signifies soil sorptivity. It is this characteristic that determines how much of the incident rainfall will run off and how much will enter the soil and either percolate downward or be evapotranspired.

Under ponded conditions, infiltration into an initially dry soil profile has a high rate early in time, decreasing rapidly and then more slowly until the rate reaches a nearly constant rate as shown on figure 11.1. As water redistributes through a soil profile, it displaces air and fills (or partially fills) the pores. The average hydraulic gradient, as well as the infiltration rate, continues to decrease during the infiltration process. The reason for the decrease in hydraulic gradient is that water is transmitted to the wetting front through an already wet-zone of soil that is continuously increasing in length as infiltration proceeds. This increases the resistance to flow and decreases the infiltration rate. It must be pointed out that this process is modified in soils that are subject to shrinking or swelling, and in materials or soils where the infiltrating liquid reacts chemically or physically with the media.

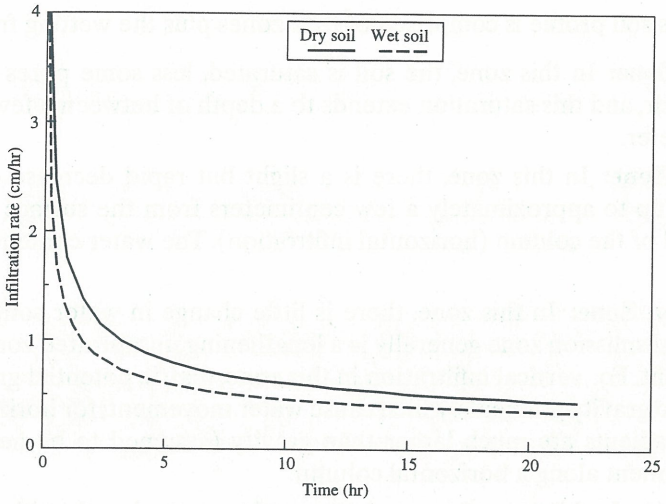

Figure 11.1 Examples of infiltration rate as a function of time and initial soil-water content

11.1 PROFILE-MOISTURE DISTRIBUTION

Consider the infiltration of water into a semi-infinite, uniform soil-profile having an initial volumetric-water content at residual saturation, θ_r. The infiltration process can be described—whether it is a horizontal or a vertical profile—by four distinct zones, as shown in figure 11.2. At the surface (or wet end of a horizontal column), the soil is nearly saturated for a few centimeters; there may be some pores where there is entrapped air. Below, or adjacent to, this saturated zone is a transmission zone where water is being transmitted to the wetting front as it moves downward (horizontally). The transmission zone is increasing in length as time goes on, with a uniform water content very near saturation. Within the wetting zone, the water content decreases until it merges into the wetting front, which forms a sharp boundary between the wet and the initially dry soil (figure 11.2). Both the wetting zone and the wetting front move continuously during the infiltration process. Thus, the wetted portion of

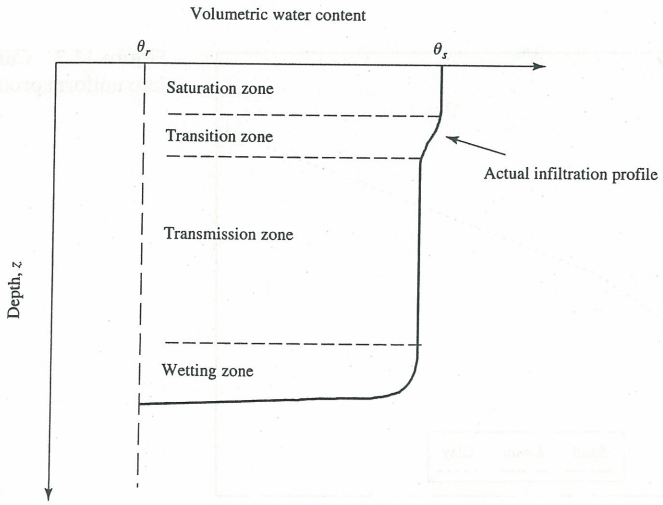

Figure 11.2 Idealized infiltration water profile distribution

the homogeneous soil profile is comprised of four zones plus the wetting front (figure 11.2):

1. **Saturated Zone:** In this zone, the soil is saturated, less some pores which may have entrapped air, and this saturation extends to a depth of between a few millimeters and one centimeter.
2. **Transition Zone:** In this zone, there is a slight but rapid decrease of water content with depth up to approximately a few centimeters from the surface (vertical infiltration) or end of the column (horizontal infiltration). The water content is still very near saturation.
3. **Transmission Zone:** In this zone, there is little change in water content from saturation. The transmission zone generally is a lengthening unsaturated zone with a uniform water content. For vertical infiltration in this zone, matric potential gradients are small compared to gravity gradients, which cause water movement; for horizontal infiltration, diffusive gradients are much larger than gravity (assumed to be negligible), causing water movement along a horizontal column.
4. **Wetting Zone:** In this zone, the water content decreases sharply with distance from the near-saturation values of the transmission zone to the initial residual-saturation value.

The wetting front is the zone of steep-water content and potential gradients, and forms a sharp boundary between the wet and dry (residual saturation) soil. Beyond the wetting front, the water content of the soil is at its initial value and there is no visible penetration of water. The moisture distribution presented in figure 11.2 is idealized, and actual moisture distributions can depart from those in figure 11.2, most likely in major qualitative ways.

Figure 11.3 shows the vertical cumulative infiltration under a thin film of water at the ground surface in three uniform soil materials consisting of a sand, a loam, and a clay. Figure 11.3 shows that at a time of 5 minutes (0.083 hours) the sand, loam, and clay profiles absorb approximately 1.3, 0.7, and 0.2 cm of water, respectively. The cumulative infiltration indicates one of the factors, soil texture, that is important in affecting infiltration rate. The factors that affect the infiltration rate can be divided into four general groups, representing **(1)** soil factors; **(2)** liquid-property factors; **(3)** rainfall or other liquid-arrival factors; and **(4)** other soil surface factors.

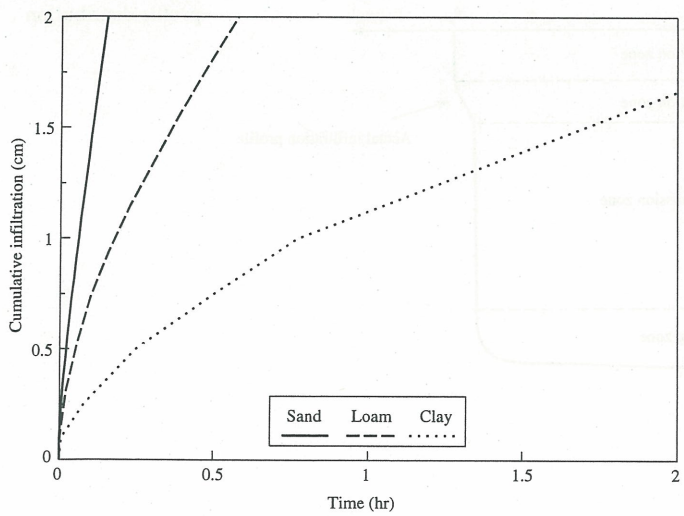

Figure 11.3 Cumulative infiltration into uniform profiles

Soil Characteristics

Soil characteristics affecting infiltration include the surface-entry characteristics and soil-transmission characteristics: texture; structure; organic matter; compaction; hydraulic conductivity; soil-water content; pore-size distribution; clay content; and behavior. Reduction of infiltration rate has been observed in soils due to surface sealing; this surface sealing can be caused by the impact of raindrops, animal activity, or vehicular traffic. The cause of the surface sealing is the movement of fine particles in between coarser particles, to form a relatively impermeable layer. Even soils exhibiting macropore flow could have the macropores clogged due to the movement of finer particles into the macropores.

When a soil material swells or increases in volume, this increase is almost always at the expense of pore volume. Macropores (non-capillary pores) (Beven and Germann 1982; Morrison 1993; Dingman 1994) can become capillary in size and smaller capillary pores are sealed. These factors affect the pore size and distribution in a soil, changing the rate of water movement and decreasing infiltration. Surface layers generally undergo larger changes in volume due to swelling and shrinking than deeper layers, even though the latter contains larger amounts of clay. Because water cannot enter a soil layer faster than it can be transmitted downward, surface conditions cannot increase the infiltration rate unless transmission characteristics of each layer of the profile are adequate. At saturation, the infiltration rate is limited to the lowest transmission rate encountered by the infiltrating water up to that time.

The total infiltration capacity of any layer depends upon its porosity, thickness, and quantity of water or other liquid present. Soil texture, structure, organic matter, root activity, and other physical properties determine the magnitude of the porosity of a given soil. Both the total porosity and the pore-size distribution determine the water-holding capacity of the soil. The initial infiltration will depend upon the volume, size, continuity, and relative stability of capillary and non-capillary pores, which provide paths for the percolating water or other liquid. Sandy materials have relatively stable pores. Well-graded silty and clayey materials, while having relatively larger pores in the dry state, on wetting, can have reduced pore sizes due to disintegration of the larger pores into smaller pores. Figure 11.3 shows the relation between total infiltration with time for a sand, loam, and clay soil representing high, moderate, and low infiltration rates, respectively. For the sand material to absorb 1 cm of water takes approximately 4 minutes; whereas for the loam material, it takes approximately 10 minutes; and for the clay material, approximately 45 minutes to absorb the same 1 cm of water.

During wetting, if air is trapped in the pores as liquid is applied from the surface to the wetting front, the entrapped air has the effect of causing a reduction on infiltration rate (Rawls et al. 1993). The reduction in rate can be large, because hydraulic conductivity is often reduced over one-half its saturated value (Bouwer 1966). The wetting front continues to advance slowly as a result of capillary forces, and the air pressure continues to increase until there is sufficient pressure to cause upward release of air through the pores holding water, and through the saturated surface layer.

The type of soil structure (e.g., fragmental, platy, cubical, blocky, prismatic, single grained, and massive), relative dimensions of structural aggregates, as well as the amount and direction of overlap of aggregates, determines the hydraulic conductivity classes. However, such secondary factors as compaction, direction of natural breakage, silt content, degree of mottling, and climatic factors are also important. Organic and inorganic fluids, along with residues, also influence the hydraulic conductivity. Dragun (1988) summarizes the effects of bulk hydrocarbons on the hydraulic conductivity and intrinsic permeability of selected soils. In general, bulk hydrocarbons result in substantial increases in hydraulic conductivity for the reasons given in the following section.

Microorganisms in the soil also are known to influence infiltration rates. Soils under prolonged saturation tend to have any entrapped air dissolved into the water, thus increasing

the infiltration rate. However, microbial-activity byproducts such as slimes, gums, and gases can clog capillary pores, resulting in decreases in infiltration rates. On the other hand, microbial decomposition of plant and animal residues can markedly increase infiltration rates; earthworms are known to increase infiltration rates in compact, fine-textured soils.

Initial volumetric-water content has a great influence on the infiltration rate. As shown in figure 11.1, the infiltration rate decreases as initial water content increases, and as the time of water or other liquid application increases, the effect of antecedent moisture decreases. Additionally, the increase in initial water content decreases the infiltration rate during the early stages of infiltration, but increases the velocity of the wetting-front advance at all times. During the first few hours of infiltration, the antecedent moisture content will probably be the major factor determining the infiltration rate of a given soil.

The initial soil-water content affects the infiltration rate in three ways: **(1)** partially full pores reduce infiltration; **(2)** wetting of an initially dry soil causes increased capillary forces that increase infiltration; however, with the increase in the depth of the wetting front, infiltration is decreased; and **(3)** wetting of the soil may cause swelling of the soil materials, which decreases infiltration.

Liquid Properties

The physical characteristics of the infiltrating fluid (e.g., water or NAPL) also affect infiltration rate. When water enters a soil, fine clays, organics, salts, and other materials contaminate the water. These suspended and dissolved materials in the infiltrating fluid not only block pores, but also may affect the viscosity, density, and surface tension of the water. Some of these materials, such as salts, can affect the swelling potential of some soils by forming complexes with colloidal materials.

The temperature, viscosity, and surface tension of the fluid affect the rate of movement of the fluid into and within the soil. The relation between the infiltration rate and factors such as temperature, viscosity, surface tension, pore size, depth of wetting, head of water, wettability of solids by solution, and density of the wetting solution, indicates that: **(1)** when temperature of the fluid is increased, there is a corresponding increase in the infiltration rate (Moore 1941); **(2)** increases in viscosity decrease the infiltration rate hyperbolically; **(3)** decreases in surface tension increase the infiltration rate linearly; **(4)** as pore size increases, infiltration rate increases parabolically; and **(5)** as depth of wetting increases, the infiltration rate decreases hyperbolically (Ghildyal and Tripathi 1987).

Rainfall or Other Liquid-Arrival Factors

The characteristics of how the fluid is deposited on the surface can have both direct and indirect effects on infiltration rate. If the maximum infiltration rate exceeds the rate at which the fluid is applied, this fluid infiltrates and a direct relation between rate of infiltration and rate of fluid application occurs. However, when fluid application rate (or application intensity) exceeds the infiltration rate, an inverse relation between application rate and infiltration rate is obtained. For example, an increase in rainfall intensity causes increased compacting forces as the raindrops hit the soil surface, thus decreasing infiltration rate. Rainfall or other fluid characteristics can also affect infiltration rate indirectly by increasing the initial soil moisture content, and the activities of earthworms and other animals.

At time $t = 0$, liquid begins arriving at the surface at a rate, w, which continues for a specified time t_w. For the idealized condition of constant liquid arrival, two cases can be considered: **(1)** the liquid-input rate at the surface is less than the saturated hydraulic conductivity; and **(2)** the liquid-input rate at the surface is greater than the saturated hydraulic conductivity. The following discussion is valid for a homogeneous layer of soil or for several layers where the underlying layers have successively higher saturated hydraulic conductivities.

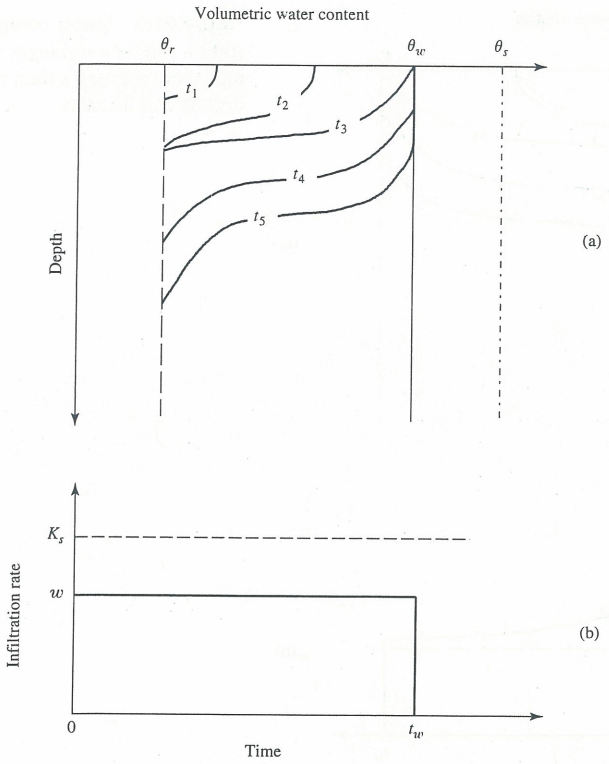

Figure 11.4 Water content profiles and infiltration rate in a soil layer where the liquid-input rate is less than the saturated hydraulic conductivity

Liquid-input rate at the surface is less than the saturated hydraulic conductivity Let us consider a thin layer of homogeneous soil at the instant that liquid input at the surface begins. If it is assumed that $w < K_s$ (figure 11.4(b)), liquid will enter this layer faster than it is leaving, resulting in an increase in volumetric-water content, θ. The increase in volumetric-water content causes an increase in hydraulic conductivity consistent with the unsaturated hydraulic-conductivity versus water-content relation for the soil. Therefore, the flux out of the layer also increases as the water content increases. However, as long as the water content in the layer is less than that at which the hydraulic conductivity, K, equals the liquid-input rate, w, the water content will continue to increase. When the water content reaches θ_w (which is less than the saturated water content, θ_s), the hydraulic conductivity is K_w, which is equal to the liquid-input rate, w, so that the rate of outflow from the layer is equal to the rate of input and there is no further change in water content for the constant liquid-input rate.

This process occurs successively in each underlying soil layer as liquid input continues. Figure 11.4a shows schematically the resulting water-content profiles in a uniform vertical soil layer. Analysis of Figure 11.4b confirms the relation that, for a liquid-input rate at the surface less than the saturated hydraulic conductivity, the infiltration rate is constant with a value of w for all time between 0 and t_w, and the infiltration rate is zero for all other times.

Liquid-input rate at the surface is greater than the saturated hydraulic conductivity When $w > K_s$, liquid still enters a thin, homogeneous surface layer faster than it is leaving, but only during the early stages of infiltration. Liquid generally arrives at each layer faster than it can be transmitted downward and initially goes into storage, increasing the water content and the hydraulic conductivity. However, because the water content cannot exceed its saturated value, θ_s, the hydraulic conductivity cannot increase beyond K_s. After the surface layer reaches saturation, liquid will accumulate on the surface and ponding will begin until surface-detention storage is satisfied. After this time, runoff will occur. Figure 11.5(a) shows the resulting water-content profiles for the case of the liquid-input rate greater than the

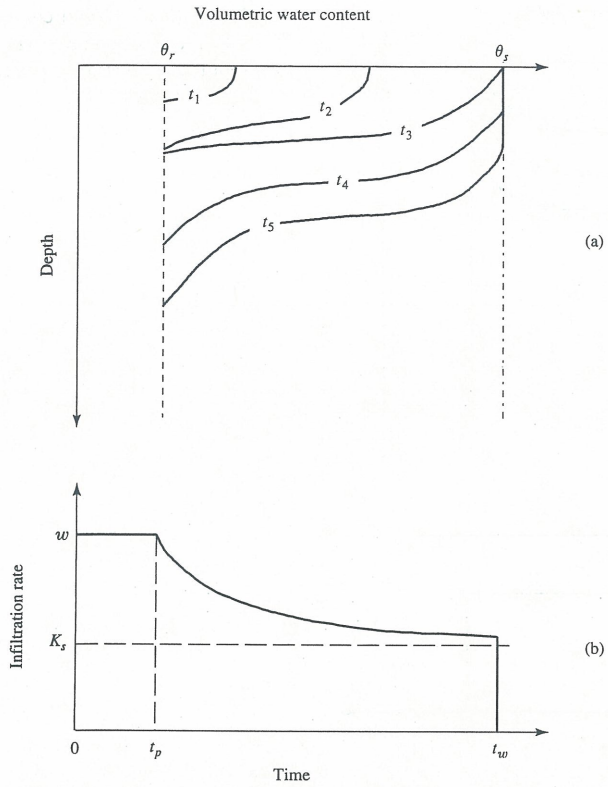

Figure 11.5 Water content profiles and infiltration rate in a soil layer where the liquid-input rate is greater than the saturated hydraulic conductivity

saturated hydraulic conductivity. The time at which the surface layer becomes saturated is called the time of ponding, t_p, which is shown schematically in Figure 11.5b. Up to the ponding time, the infiltration rate is equal to the liquid-input rate, w. As liquid input continues after the time of ponding, infiltration continues but at an asymptotically decreasing rate towards K_s (figure 11.5b), until cessation of liquid input.

Other Soil-Surface Factors

Surface slope, vegetative cover, and roughness all have an effect upon the infiltration rate (Ghildyal and Tripathi 1987). Steep, smooth slopes with little vegetative cover allow little time for infiltration; on flatter, rougher slopes with vegetation, infiltration is encouraged. Clearly, one of the factors governing infiltration is time available for the process to occur. Thus, surface conditions which slow runoff increase the infiltration volume and rate, other factors being equal. Vegetation can be a particularly important factor, because vegetative cover tends to retard surface-water runoff, allowing time for infiltration to occur. Additionally, vegetation reduces the compaction of the soil surface due to influence of falling raindrops. The plant roots may increase hydraulic conductivity of the surface layers, thereby increasing infiltration. Types of natural and cropping vegetative cover have a significant effect on infiltration (Brakensiek and Rawls 1988; Branson et al. 1981).

11.2 INFILTRATION THEORIES

As shown in chapter 8, combining Darcy's law with the one-dimensional continuity equation results in the one-dimensional Richards' equation for vertical flow in an unsaturated soil.

No known closed-form analytical solutions exist for Richards' equation in layered soil, unless it is assumed that the flux rate, q, is constant (see chapter 13). For nonlayered soil with

a uniform initial-water content, some closed-form solutions for variable flux rates (infiltration rates) are available. These physically based solutions include those by Green and Ampt (1911), Philip (1957a, b, c, d), Morel-Seytoux and Khanji (1974), and Smith and Parlange (1978). Solutions to Richards' equation can also be obtained numerically under appropriate boundary and initial conditions.

In addition to physically based, closed-form solutions to Richards' equation for homogeneous soils, several empirical equations are often used in operational hydrology. These equations, such as the Horton equation (Horton 1939; 1940), Holtan equation (Holtan 1961), and Kostiakov equation (Kostiakov 1932), relate measured infiltration rate or cumulative-infiltration to elapsed time modified by various soil and vegetation parameters. These parameters have to be obtained by fitting them to measured data. These infiltration theories are reviewed in more detail in the following sections.

Green–Ampt Approach

One of the earliest physically based approaches to infiltration of water into soils was formulated by Green and Ampt (1911), for soils that exhibit a sharp wetting front. A sharp wetting front is most common in soils having uniform pore shapes and being generally coarse-textured. The following assumptions for the Green–Ampt model permit an analytical solution to the infiltration equation: **(1)** the soil under consideration is homogeneous with respect to water retention and transmission properties; **(2)** a distinct and precisely definable wetting front exists; **(3)** matric suction at the wetting front remains constant throughout infiltration; and **(4)** the soil is uniformly wet behind the wetting front.

For horizontal infiltration into a uniform soil column where gravitational forces can be neglected, a Darcy-type equation can be written as:

$$i = \frac{dI}{dt} = K_s \frac{\psi_0 - \psi_f}{L_f} \tag{11.1}$$

where i is the infiltration rate (flux rate) into the soil and through the transmission zone, I is the cumulative infiltration, K_s is the saturated hydraulic conductivity of the transmission zone, ψ_0 is the saturated suction (matric potential = 0), ψ_f is the effective suction at the wetting front, and L_f is the distance from the soil surface to the wetting front (length of the total infiltration zone). Because $\psi_0 - \psi_f$ is constant and is independent of time and space as long as the soil surface is maintained at a matric potential of zero and the ponding depth is negligible, equation 11.1 can be rewritten as

$$\frac{dI}{dt} = K_s \frac{\Delta\psi}{L_f} \tag{11.2}$$

where $\Delta\psi$ is the change in potential from the soil surface to the wetting front. Equation 11.2 also indicates that the infiltration rate i is a linear inverse function of the total infiltration zone length, L_f. Because the distance from the surface to the wetting front is uniform, cumulative infiltration I can be given by

$$I = L_f(\theta_t - \theta_i) \tag{11.3}$$

where θ_t is the transition-zone volumetric water content during infiltration, and θ_i is the initial soil volumetric water content. For the special case where θ_t is the volumetric water content at saturation (porosity) and θ_i is zero, then cumulative infiltration in equation 11.3 is given by

$$I = \phi L_f \tag{11.4}$$

where ϕ is the effective porosity. Thus,

$$\frac{dI}{dt} = (\theta_t - \theta_i)\frac{dL_f}{dt} \tag{11.5}$$

where dL_f/dt is the rate of advance of the wetting front during infiltration. It should be recognized that

$$K_s \frac{\Delta\psi}{L_f} = K_s \frac{\Delta\theta\,\Delta\psi}{I} \tag{11.6}$$

or the infiltration rate i is an inverse function of the cumulative infiltration I.

Substituting the value of L_f in equation 11.3 into equation 11.2 gives

$$\frac{dI}{dt} = K_s \frac{\Delta\psi\,(\theta_t - \theta_i)}{I} \tag{11.7}$$

Rearranging equation 11.7 and integrating

$$\int I\,dI = [K_s\,\Delta\psi\,(\theta_s - \theta_i)] \int dt \tag{11.8}$$

or

$$\frac{I^2}{2} = K_s\,\Delta\psi\,(\theta_t - \theta_i)t + C \tag{11.9}$$

where C is the constant of integration.

For typical initial conditions $t = 0$ and $I = 0$, and therefore $C = 0$. The cumulative infiltration I is then given by

$$I = [2K_s\,\Delta\psi\,(\theta_t - \theta_i)]^{1/2}\,t^{1/2} \tag{11.10}$$

Writing $(\theta_t - \theta_i)$ as $\Delta\theta$, equation 11.10 can be expressed as

$$I = \Delta\theta\,(2\tilde{D}t)^{1/2} \tag{11.11}$$

where $\tilde{D}$ is the effective diffusivity of the draining soil profile, given by

$$\tilde{D} = K_s \frac{\Delta\psi}{\Delta\theta} \tag{11.12}$$

It should be noted that the quantities in the brackets on the right-hand side of equation 11.10 are constant for all times greater than zero. This implies that the relation between cumulative infiltration I and $t^{1/2}$ will be linear, with the straight line passing through the origin and having a constant slope, S, given by

$$S = [2K_s\,\Delta\psi\,(\theta_t - \theta_i)]^{1/2} = \Delta\psi\,(2\tilde{D})^{1/2} \tag{11.13}$$

where S is called the sorptivity. Differentiating equation 11.13 gives an expression for infiltration rate i

$$i = \frac{dI}{dt} = \left[\frac{1}{2}K_s\,\Delta\psi\,(\theta_t - \theta_i)\right]^{1/2} t^{-1/2} \tag{11.14}$$

Equations 11.10 and 11.14 show that the cumulative infiltration I increases, whereas the infiltration rate i decreases linearly with the square root of time.

Gravitational forces (vertical infiltration) can be taken into account by adding the distance from the soil surface to the wetting front to equation 11.1, which is the Green–Ampt

model for horizontal infiltration, or

$$i = \frac{dI}{dt} = K_s \frac{\psi_b + L_f - \psi_f}{L_f} \tag{11.15}$$

which can be rewritten as

$$i = \frac{dI}{dt} = K_s \left[1 + \frac{\psi_b - \psi_f}{L_f}\right] \tag{11.16}$$

In this case, ψ_b is defined as the bubbling pressure (potential), which is the potential at which the largest pore begins to drain.

From equation 11.16, it is apparent that the infiltration rate i is maximum early in the infiltration process, when the length of the total infiltration zone L_f is minimum, and decreases as L_f increases. Also, i approaches a constant value K_s as $t \to \infty$, for which L_f becomes very large, or

$$i(t = \infty) = K_s \tag{11.17}$$

If L_f in equation 11.3 is substituted into equation 11.16, we obtain the common form of the Green–Ampt equation

$$i = K_s \left(1 + \frac{(\theta_t - \theta_i)\,\Delta\psi}{I}\right) \tag{11.18}$$

If equation 11.5 is substituted into equation 11.16, we obtain

$$(\theta_t - \theta_i)\frac{dL_f}{dt} = K_s \left(1 + \frac{\psi_b - \psi_f}{L_f}\right) \tag{11.19}$$

Rearranging the terms and integrating equation 11.19 gives

$$\frac{K_s}{(\theta_t - \theta_i)} \int dt = \int \frac{L_f}{(\psi_b - \psi_f) + L_f} dL_f \tag{11.20}$$

or

$$\frac{K_s t}{(\theta_t - \theta_i)} = (\psi_b - \psi_f) + L_f - (\psi_b - \psi_f) \ln (\psi_b - \psi_f + L_f) + C \tag{11.21}$$

where C is the constant of integration that can be evaluated for the initial conditions of $t = 0$ and $L_f = 0$, so that

$$C = -(\psi_b - \psi_f) + (\psi_b - \psi_f) \ln (\psi_b - \psi_f) \tag{11.22}$$

and equation 11.21 finally becomes

$$\frac{K_s t}{(\theta_t - \theta_i)} = \left[L_f - (\psi_b - \psi_f) \ln \left(1 + \frac{L_f}{\psi_b - \psi_f}\right)\right] \tag{11.23}$$

Equation 11.23 relates the total infiltration depth to the wetting front at time t to the cumulative infiltration volume. In general, as time increases, L_f increases such that at very long times, equation 11.23 can be approximated by

$$K_s t = (\theta_t - \theta_i) L_f + A \tag{11.24}$$

where

$$A = -(\theta_t - \theta_i)\left[(\psi_b - \psi_f) \ln \left(1 + \frac{L_f}{\psi_b - \psi_f}\right)\right] \tag{11.25}$$

From equation 11.3, equation 11.24 can also be written as

$$I = K_s I - A \tag{11.26}$$

where A changes much more slowly as L_f becomes very large. The infiltration rate i at large L_f thus becomes

$$i = K_s \tag{11.27}$$

The Green–Ampt model is satisfactory for both unponded and ponded surface conditions. For infiltration under ponded conditions, the soil in the total infiltration zone is nearly saturated. This near-saturation condition develops a viscous resistance to air flow, which reduces infiltration rate. To account for this effect, Morel-Seytoux and Khanji (1974) introduced a correction factor to the Green–Ampt equation for a homogeneous soil (discussed later in this section).

To apply the Green–Ampt model, the saturated hydraulic conductivity K_s, suction at the wetting front ψ_f, initial volumetric water content θ_i, and transition-zone volumetric water content θ_t all must be measured or estimated. Obviously these variables can be calculated by fitting them to experimental infiltration data; however, other data may also be readily available that can be used.

It can be assumed that θ_t is approximately equal to porosity ϕ, which can be obtained from other geotechnical tests or calculated from bulk density and particle density. K_s can be obtained from laboratory tests, as can θ_i. If moisture-characteristic curve data are available for a specific soil, ϕ should be available from these data. Regression equations available from Rawls and Brakensiek (1983) or Rawls et al. (1993) can also be used to estimate detailed soil properties.

The Green–Ampt effective suction at the wetting front can be estimated from Rawls et al. (1993) and the Brooks–Corey variables (Brooks and Corey 1964) as

$$\psi_f = \frac{2 + 3\lambda}{1 + 3\lambda} \frac{\psi_b}{2} \tag{11.28}$$

where ψ_f is the Green–Ampt effective suction at the wetting front, λ is the Brooks–Corey pore-size distribution index, and ψ_b is the Brooks–Corey bubbling pressure (suction). Both λ and ψ_b are variables determined by fitting a Brooks–Corey relation to moisture-characteristic curve data. The methodology for estimating these two fit-variables is detailed in chapter 13. Rawls and Brakensiek (1983) and Rawls et al. (1993) present regression equations for estimating λ and ψ_b from a soil sample if the percent sand, percent clay, and porosity of the sample are known.

Figure 11.6 is an example of the Green–Ampt model to calculate infiltration rate (equation 11.18) versus time for various assumed cumulative infiltration values I for two different soils. A river sand, having $\Delta\psi = 16$ cm, $K_s = 26.4$ cm/hr, $\theta_t = 0.39$, and $\theta_i = 0.20$; and the other a Laveen Loam, having $\Delta\psi = 25$ cm, $K_s = 0.45$ cm/hr, $\theta_t = 0.38$ and $\theta_i = 0.30$. In this case, I was assumed and the time t was calculated as the ratio of the initially assumed cumulative infiltration to the infiltration rate calculated by equation 11.18. The coarser-grained river sand experiences larger values of cumulative infiltration and higher initial and final infiltration rates.

Horton and Kostiakov Equations

Horton (1939; 1940) proposed an empirical formula for infiltration, based upon the many natural processes that move spontaneously to their final value at a rate determined by the difference between their initial and final values. Horton's derivation of infiltration as a function of time began with

$$\frac{di}{dt} = -k(i - i_f) \tag{11.29}$$

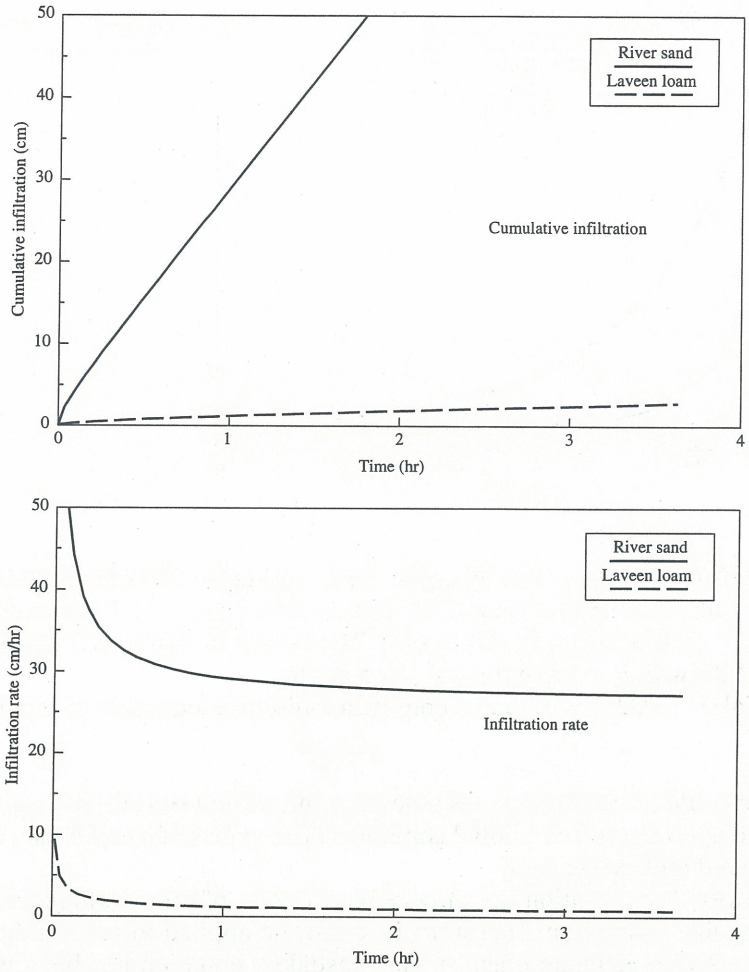

Figure 11.6 Green–Ampt cumulative infiltration, and infiltration rates for two different soils

where i is the infiltration rate, i_f is the final (constant) infiltration rate, k is a proportionality constant ($k > 0$) dependent on the soil type and vegetative cover, and t is the time since the liquid input began. The negative sign in equation 11.29 indicates that infiltration decreases toward its final constant value. If the initial infiltration rate is i_o at zero time, then equation 11.29 can be integrated to yield

$$\ln \frac{(i - i_f)}{(i_o - i_f)} = -kt \tag{11.30}$$

or, solving for i

$$i = i_f + (i_o - i_f)\, e^{-kt} \tag{11.31}$$

It is clear from equation 11.31 that as $t \to \infty$, i approaches a constant rate, i_f at $k > 0$. Cumulative infiltration can be found by integrating equation 11.31 and applying the initial conditions of $I = 0$ when $t = 0$. The resulting cumulative infiltration is

$$I = i_f t + \frac{i_o - i_f}{k}(1 - e^{-kt}). \tag{11.32}$$

Values of i_o, i_f, and k depend upon soil and vegetative cover complexes. According to Skaggs and Khaleel (1982), typical values for agricultural soils range from approximately 30

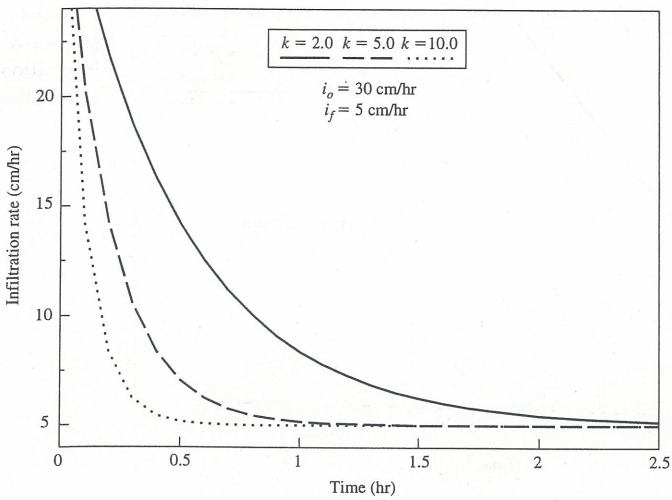

Figure 11.7 Variation of k on Horton infiltration rate

to 90 cm/hr for i_o; less than 1 to 30 cm/hr for i_f; and up to 50/hr for k. Values of i_o, i_f, and k should be evaluated using observed infiltration data. Figure 11.7 shows changes in infiltration rate for various assumed values of k. The curves in figure 11.7 were calculated using equation 11.30, with $i_o = 30$ cm/hr and $i_f = 5$ cm/hr.

Kostiakov (1932) proposed an empirical infiltration equation of the form

$$I = at^b \tag{11.33}$$

where I is cumulative infiltration, t is time since infiltration started, and a and b are constants that depend upon the soil and initial conditions. The values of a and b may only be estimated using observed infiltration data.

The Kostiakov equation can only be used if a set of observed infiltration data is available for variable estimation. Therefore, it cannot be applied to soil conditions which differ from those used to estimate a and b. The Kostiakov equation has been used primarily for analysis of irrigation applications (Rawls et al. 1993).

Holtan Model

Holtan (1961) presented an empirical infiltration equation, based on the concept that the infiltration rate is proportional to the unfilled pore volume of a soil. Holtan's equation was developed by assuming that the unfilled pores included surface-connected porosity and the effects of root paths, which are probably the most important features affecting infiltration rate. Holtan's (1961) original equation was of the form

$$i = aI_p^n + i_f \tag{11.34}$$

where i is the infiltration rate, i_f is the final (constant) infiltration rate, I_p is the unfilled capacity of the soil to store water, and a and n are constants. The Holtan model has the advantage over the Horton model in that it can describe infiltration rate and the recovery of infiltration capacity during periods of little or no rainfall.

Holtan et al. (1975) modified equation 11.34 to give

$$i = GAI_p^{1.4} + i_f \tag{11.35}$$

where G is the growth index of the vegetative cover in percent maturity, varying from 0.1 to 1.0 during the growing season; A is the infiltration capacity of available storage and is an

index representing surface-connected porosity and the density of plant roots which affect infiltration; I_a is the available storage in the soil-surface layer (A horizon); and n is now held constant at 1.4. The value of I_a ranges from zero to a maximum of the available water-holding capacity of the soil. Values of water-holding capacity are given for many soils by Rawls et al. (1993). Values of the vegetative parameter A are given in table 11.1 (Frere, Onstad, and Holtan 1975). Musgrave (1955) provided values of i_f that were related to U.S. Soil Conservation Service (SCS) hydrologic soil groups. These values of i_f are presented in table 11.2, along with the SCS definitions for each hydrologic soil group (SCS 1980).

TABLE 11.1 Estimates of Vegetative Parameter A in the Holtan Infiltration Equation

	Basal area rating* (in.$^{1.4}$/hr)	
Land use or cover	Poor condition	Good condition
Fallow†	0.10	0.30
Row crops	0.10	0.20
Small grains	0.20	0.30
Hay (legumes)	0.20	0.40
Hay (sod)	0.40	0.60
Pasture (bunch grass)	0.20	0.40
Temporary pasture (sod)	0.20	0.60
Permanent pasture (sod)	0.80	1.00
Woods and forests	0.80	1.00

Source: Data from Frere, Onstad, and Holtan (1975).
*Adjustments needed for "weeds" and "grazing."
†For fallow land only, poor condition means "after row crop" and good condition means "after sod."

TABLE 11.2 Final Infiltration Rates by SCS Hydrologic Soil Group for the Holtan Infiltration Equation

SCS Hydrologic Soil Group[1]	i_f (cm/hr)
A	0.76
B	0.38–0.76
C	0.13–0.38
D	0.0–0.13

Sources: Data from Musgrave (1955) and SCS (1980).
[1]**Group A** soils have low runoff potential and high infiltration rates even when thoroughly wetted. They consist mainly of deep, well-to-excessively drained sand or gravel. The USDA soil textures normally included in this ground are sand, loamy sand, and sandy loam. These soils have a transmission rate greater than 0.76 cm/hr.
Group B soils have moderate infiltration rates when thoroughly wetted and consist mainly of moderately deep to deep, moderately well to well-drained soils with moderately fine to moderately coarse textures. The USDA soil textures normally included in this group are silt loam and loam. These soils have transmission rate between 0.38 and 0.76 cm/hr.
Group C soils have low infiltration rates when thoroughly wetted and consist mainly of soils with a layer that impedes downward movement of water and soils with moderately fine to fine texture. The USDA soil textures normally included in this group is sandy clay loam. These soils have a transmission rate between 0.13 and 0.38 cm/hr.
Group D soils have high runoff potential. They have very low infiltration rates when thoroughly wetted and consist mainly of clay soils with a high swelling potential, soils with a permanent high-water table, soils with a claypan or clay layer at or near the surface, and shallow soils over a nearly impervious material. The USDA soil textures normally included in this group are clay loam, silty clay loam, sandy clay, silty clay, and clay. These soils have very low rate of water transmission (0.0 to 0.13 cm/hr).

Philip Model

Using a series approximation, Philip (1957a, b, c, d) found the cumulative infiltration I, in a horizontal, semi-infinite column to be

$$I = St^{1/2} + (A_2 + K_o)\,t + A_3\,t^{3/2} + A_4\,t^2 + \cdots + A_m\,t^{m/2} + \cdots \tag{11.36}$$

where $S, A_2 + K_o, A_3, A_4, \ldots$ are functions of volumetric water content that are the solutions of a series of ordinary equations. Philip found that the power series in $t^{1/2}$ given by equation 11.36 converged for all except very large t. Philip (1957d) called S the sorptivity, which he claimed was a property of the medium. For a uniform, semi-infinite horizontal-soil column having a sharp wetting front, the sorptivity S is approximately given by

$$S \approx \frac{(\theta_s - \theta_i)x}{t^{1/2}} \tag{11.37}$$

where x is the horizontal distance of the wetting front from the end of the column, θ_i is the initial volumetric water content of the column, θ_s is the saturated volumetric water content behind the wetting front, and t is the time since water started entering the column.

The horizontal infiltration rate i can be determined by taking the derivative of equation 11.36, or

$$i = \frac{dI}{dt} = \frac{1}{2}St^{-1/2} \tag{11.38}$$

where only the first term in equation 11.36 is significant. As with other physically based infiltration equations, water is transferred to the wetting front through a wet zone that is continuously increasing in length. This increases the resistance to flow and decreases the infiltration rate. The equation of cumulative infiltration I can be used to determine sorptivity S, provided the infiltration is known at some time from field or laboratory experiments.

Philip (1957d) provided an approximate solution to the vertical-infiltration equation for a homogeneous soil with water ponded on the surface as

$$I = St^{1/2} + At \tag{11.39}$$

where I is the cumulative infiltration, S is sorptivity, t is time, and A is a soil parameter. The value of A is related to the hydraulic conductivity of the soil. For a saturated soil surface, A is identical to the saturated-hydraulic conductivity K_s. If the soil surface does not have a thin film of ponded water, then A is equal to the unsaturated hydraulic conductivity K of the transmission zone.

The equation for vertical infiltration rate can be obtained by differentiating equation 11.39, or

$$i = \frac{dI}{dt} = \frac{1}{2}St^{-1/2} + A \tag{11.40}$$

where A is equal to K_s if water is ponded on the surface and equal to K, otherwise.

In the Philip model, the variables S and A can be evaluated from experimental infiltration data using best-fit regression techniques; however, these variables may also be estimated from laboratory data using approximations presented by Rawls et al. (1993). Sorptivity S in the Philip model can be approximated using an equation originally developed by Youngs (1964)

$$S = [2(\theta_t - \theta_i)K\psi_f]^{1/2} \tag{11.41}$$

where ψ_f is the Green–Ampt effective suction at the wetting front given by equation 11.31, θ_t is the transition-zone volumetric water content which can be taken as the soil porosity if a thin film of water is ponded on the surface, and θ_i is the initial water content. For

homogeneous soil conditions with no macropore flow, surface crust, or vegetative cover, the value of K in equation 11.41 can be assumed to be the saturated hydraulic conductivity K_s. Bouwer (1966) suggests that the value of K should be the hydraulic conductivity at residual air saturation, or a value of 0.5 K_s. Other conditions affecting K are discussed in following sections. The variable A in Philip's model was found by Youngs (1964) to range from 0.33 K_s to K_s, with K_s being the recommended value (Rawls et al. 1993).

Morel-Seytoux and Khanji Model

Morel-Seytoux (1973) was the first to show the important effect of air movement on water infiltration into an initially dry soil, under ponded conditions. Morel-Seytoux and Khanji (1974) recognized, as have others, that the Green–Ampt equation for infiltration could lead to errors of prediction by an excess of between 10 and 70 percent, especially when infiltration was occurring under ponded conditions. In the case of ponded conditions, the soil in the transmission zone (see figure 11.2) is nearly saturated, and develops a viscous resistance to air flow; this resistance reduces the infiltration rate. To correct for this, Morel-Seytoux and Khanji (1974) found it necessary to introduce a viscous correction factor, β. No particular pattern of β emerges as a function of soil type. Morel-Seytoux and Khanji (1974) suggest that the values of infiltration rate given by the Green–Ampt model (equation 11.18) be divided by β to give

$$i = \frac{K_s}{\beta}\left(1 + \frac{(\theta_t - \theta_i)(H_o + \Delta\psi)}{I}\right) \tag{11.42}$$

where H_o is the depth of ponded water.

The correction factor, β, varies with the soil type and ponding depth, ranging from approximately 1.1 to 1.7, with an average of 1.4. This factor should be used to reduce the Green–Ampt infiltration rate by dividing that rate by the correction factor, when entrapped air in the soil is a significant factor.

Smith–Parlange Model

Smith and Parlange (1978) considered two extreme cases concerning the behavior of unsaturated hydraulic conductivity K, near saturation during infiltration. In one case they assume that K varies slowly near saturation and leads to an expression for ponding time and infiltration rate. For initially ponded conditions (a thin film of water on the soil surface), the ponding time was zero and Smith and Parlange's model resulted in the Green–Ampt model

$$i = K_s\left(1 + \frac{S}{K_s I}\right) \tag{11.43}$$

where S is the sorptivity previously given by equation 11.13.

In the other second extreme, Smith and Parlange (1978) assumed that near saturation K varies exponentially. This model will hold for both the non-ponding and ponding cases, and for ponded conditions the expression for infiltration rate is given by

$$i = \frac{K_s \exp\left(\frac{IK_s}{S}\right)}{\exp\left(\frac{IK_s}{S - 1}\right)} \tag{11.44}$$

Equations 11.43 and 11.44 both use only two parameters, the saturated hydraulic conductivity and the sorptivity. As seen above both of these parameters are related to measurable soil properties based upon either field or laboratory tests.

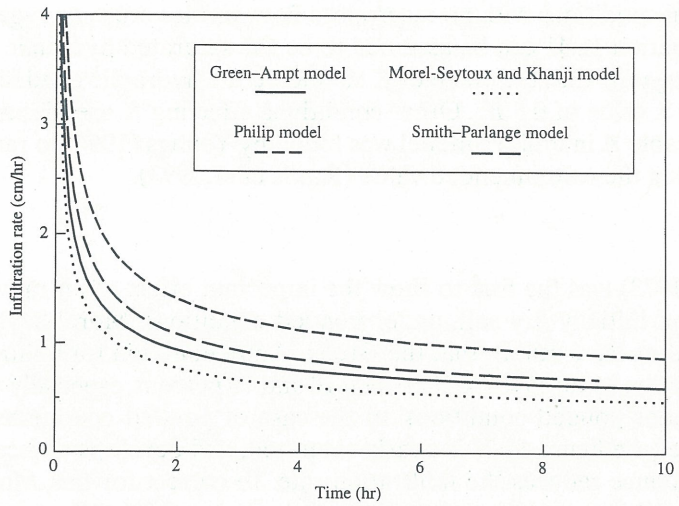

Figure 11.8 Comparison of physically based infiltration models for a Laveen loam

Comparison of the Various Physically Based Infiltration Models

Figure 11.8 shows the infiltration rates versus time for the Green–Ampt, Philip, Morel-Seytoux and Khanji, and Smith and Parlange models, for a Laveen loam having the properties presented above. The curves in figure 11.8 assume that ponding is immediate, but that the depth of ponding is infinitesimally small. A value of β equal to 1.35 was assumed for the Morel-Seytoux and Khanji model.

The Philip model appears to predict the highest infiltration rates, whereas the Morel-Seytoux and Khanji model predicts the lowest. The other two models predict between these two extremes. All models appear to provide acceptable predictions for the Laveen loam.

11.3 EFFECTS OF MACROPOROSITY

Non-capillary pores (macropores) have been categorized by Beven and Germann (1982) into four morphological groups: **(1)** pores formed by soil fauna; **(2)** pores formed by plant roots; **(3)** crack and fissures; and **(4)** natural soil pipes. A single dead-root channel or worm hole can govern both the drainage of water and air movement through a block of soil. Beven and Germann (1982) observed that there should be no doubt that, under saturated conditions, water will move through the large pores. Because water flowing through macropore channels encounters minor viscous resistance, macropores have large conductivities.

Kirkby (1988) defined macropores as being at least one order-of-magnitude (10 times) larger than indigenous pores. Even though the porosity contributed by macropores to the total soil porosity is usually small (Watson and Luxmoore 1986), they may transmit more than 70 percent of the total water-flux at saturation. Typically, macropores constitute 0.001 to 0.05 percent (1 to 50 per 10,000 volumes) of total soil volume (Morrison 1993). However, many questions remain as to how and when flow occurs in macropores, and how these pores interact with the surrounding soil matrix under unsaturated conditions.

Rawls et al. (1993) provide two approaches to modeling infiltration with macropores. One approach is to adjust the saturated hydraulic conductivity to account for the macropores. A second approach is to consider the soil as two domains comprised of the macropores and the soil matrix, with an interaction between these two domains.

Adjustment of the saturated hydraulic conductivity to account for macroporosity is a practical approach, providing an effective hydraulic conductivity with macropores as the

product of the saturated-hydraulic conductivity K_s, without macropores times a macroporosity factor (Rawls, Brakensiek, and Savabi 1989; Brakensiek and Rawls 1988)

$$K_{mp} = AK_s \tag{11.45}$$

where K_{mp} is the effective hydraulic conductivity with macropores, K_s is the saturated hydraulic conductivity without macropores, and A is the macroporosity factor. Rawls et al. (1993) present two macroporosity factors A for two different land uses. For areas that do not undergo mechanical disturbance on a regular basis—such as rangeland—the prediction equation for the undisturbed macroporosity factor is

$$A = \exp(2.82 - 0.099PS + 1.94\rho_b) \tag{11.46}$$

where PS is the percent sand (2.0 to 0.05 mm) for the less-than-2.0-mm fraction of a given soil and ρ_b is the dry-bulk density of the less-than-2.0-mm fraction of a given soil. For areas that undergo mechanical disturbance on a regular basis—such as cultivated land—the prediction equation for the disturbed macroporosity factor is

$$A = \exp(0.96 - 0.032PS + 0.04PC - 0.032\rho_b) \tag{11.47}$$

where PC is the percent clay (< 0.002 mm) fraction for the less-than-2.0-mm fraction of a given soil and the other variables are as defined above. The values of A given by equations 11.49 and 11.47 are constrained to be not less than 1.0 (Rawls et al. 1993).

The more physically based approach to macropore effects on infiltration is that, under rainfall or spill conditions, the flow into macropores begins only after ponding on the soil surface. Infiltration into the soil matrix before and after ponding can be modeled by the physically based approaches given in section 11.2. After ponding, the free fluid available at the surface is allowed to flow into the macropores. The flow in macropores can be adsorbed by the drier soil matrix via diffusion below the transient wetting front, or laterally. The lateral infiltration begins at the uppermost point below the soil matrix wetting front, and proceeds downward until the available fluid is absorbed or the lowest point of interest is reached.

11.4 LAYERED SOILS

Water cannot enter the soil at a faster rate than it is transmitted downward. Therefore, soil-surface conditions cannot increase infiltration rate unless the transmission-zone characteristics of each layer of the system are adequate. The infiltration rate of the surface layer can be low due to compaction induced by traffic or heavy machinery, raindrop impact, or the nature of the soil texture and structure, this compaction is often called "crusting" and will be discussed in the following section.

At saturation, the rate of infiltration is limited to the lowest transmission rate encountered by infiltrating water (or other fluid), up to that time. In a soil-layered profile, consider three layers: A, B, and C. If the B-layer has a rate of transmission lower than that of the A- and C-layers, the initial infiltration will be governed by the transmission rate of the A-layer until it is saturated, and later by the B-layer. Because the B-layer has a lower transmission rate than the C-layer, the infiltration into C will be limited by the B-layer, so C may not reach saturation.

It is interesting to note that the infiltration rate into a layered soil (exclusive of crusting) generally decreases when a boundary between layers is encountered, whether the underlying layer is sand or clay. This phenomenon is shown graphically in figure 11.9 (Miller and Gardner 1962). When the wetting front encounters a smaller-pored material—such as a clay layer—than that in which it has been moving, the smaller pores begin to fill rapidly because of their greater attraction for water (larger negative matric potential). As the wetting

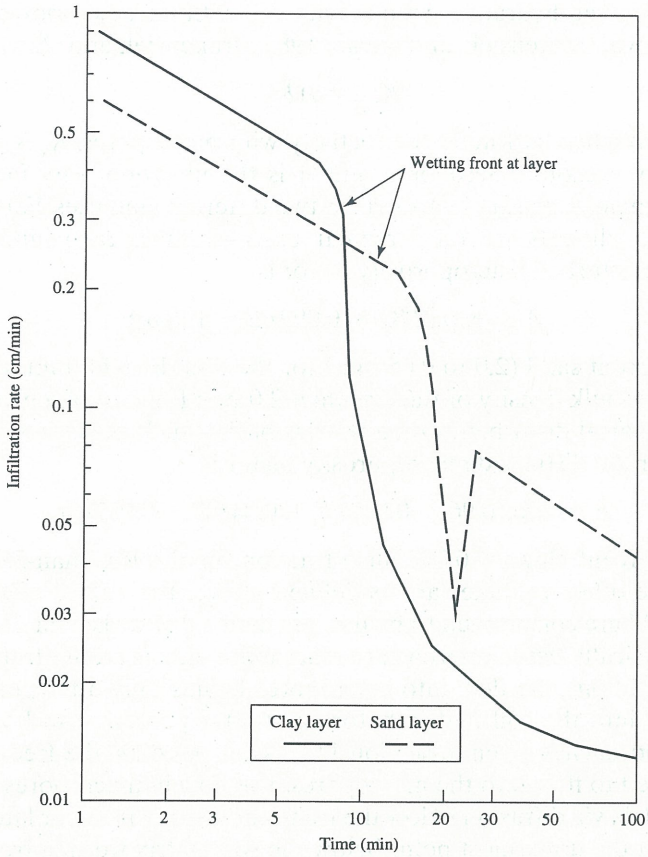

Figure 11.9 Infiltration rate into a palouse silt loam underlain by a clay and sand layer

front advances into the clay layer, water is transmitted through the smaller pores that have filled. For clayey soils, resistance to flow is often large due to the small pores, and can be so great that flow rates are markedly reduced. Figure 11.9 shows over an order-of-magnitude decrease in infiltration rate when the wetting front encounters the clay layer, with a continued decrease (but not as rapid) as time goes on.

When the wetting front (after moving through a relatively small-pored material) encounters a larger-pored material, the pore sizes capable of holding water at the matric potentials existing in the small-pored material are few in number. Before the wetting front can advance, the matric potentials in the small-pored material must be equal to those in a majority of the large-pored material, so that these larger pores may begin filling with water. However, some water continues to enter the larger-pored material, in response to a small potential gradient. Figure 11.9 shows that when the wetting front encounters the sand layer, the infiltration rate immediately decreases, but not as much as for the clay layer. As the overlying smaller-pored material increases in saturation (and decreases in negative matric potential), the larger pores in the sand begin to fill and the infiltration rate rebounds, but not to the original pre-encounter rate. The infiltration rate then resumes at a rate determined by the overlying smaller-pored—and presumably smaller-hydraulic conductivity—material. The relative size of the pores in the coarse material, when compared to the size of the pores in the overlying layer, determines the degree to which infiltration is affected (Miller and Gardner 1962).

The effect of layers of larger-pored materials on infiltration should be somewhat similar, regardless of the direction of flow, and should vary only in magnitude. This is because of the effects of gravity on downward-versus-downward or -horizontal infiltration. Therefore,

data obtained for downward wetting can be used to infer similar infiltration patterns, if upward or horizontal layering were present instead.

The Green–Ampt equations 11.18 and 11.23 can be modified to describe infiltration into layered materials if the saturated hydraulic conductivity of the successive layers decreases with depth (Childs and Bybordi 1969; Hachum and Alfaro 1980). If the wetting front is in the top layer, no changes in equations 11.18 or 11.23 are needed. Rawls et al. (1993) indicate that after the wetting front enters the second layer, the saturated-hydraulic conductivity can be set to the harmonic-mean hydraulic conductivity, or

$$K_{s_h} = \sqrt{K_{s_1} K_{s_2}} \tag{11.48}$$

for wetted depths of the first and second layers, respectively. Additionally, the change in matric potential $\Delta\psi$ is set to that of the second layer. This is valid both with and without ponding, if modifications in $\Delta\psi$ are made for the ponding depth. This same principle can be used for three or more layers as well.

For a layered soil in which the saturated hydraulic conductivity of a lower layer is greater than that of an overlying layer (typical of the crusted condition), no simple variable-substitution method for the Green–Ampt equations is available after the wetting front enters the second (higher-K_s) layer. An approximation for such cases is available by assuming that infiltration through the higher-K_s layer continues to be governed by the harmonic mean of the upper layers (Rawls et al. 1993). As we see under a special case in the next section, the Green–Ampt equations can be modified to account for a crust at the surface.

11.5 CRUSTED SOILS

Crusted soils are a special case of layered soils. Often the crust is very thin, between 1.5 and 3.0 mm (Rawls et al. 1993). Assuming that the depth of ponded water on top of the crust is negligible, the horizontal-infiltration rate into soils with a surface crust can be written as

$$i = \frac{dI}{dt} = K_s\left(\frac{\psi_f - \psi_i}{L_f}\right) \tag{11.49}$$

where K_s is the saturated hydraulic conductivity of the transmission zone beneath the crust; ψ_f is the effective suction at the wetting front; and ψ_i is the effective suction at the interface of the crust and the soil. Note that $\psi_f - \psi_i$ is the reduced driving force for infiltration into the soil beneath the crust. L_f is still defined as the distance from the soil surface to the wetting front if the crust thickness is small.

Alternatively, equation 11.49 can be written as

$$\frac{dI}{dt} = \frac{\psi_f}{R_e + R_s} \tag{11.50}$$

where R_e is the hydraulic resistance of the crust, and R_s is the hydraulic resistance of the sub-crust transmission zone. R_s can be given, for a thin crust, by

$$R_s = \frac{L_f}{K_s} \tag{11.51}$$

Combining equations 11.50 and 11.51 gives

$$i = \frac{dI}{dt} = \frac{K_s\psi_f}{K_s R_e + L_f} \tag{11.52}$$

Substituting L_f from equation 11.3 into equation 11.52 and rearranging, we obtain

$$(I + K_s R_e\,\Delta\theta)\,dI = K_s\psi_f\,\Delta\theta\,dt \tag{11.53}$$

where $\Delta\theta$ is the difference in volumetric water content in the transition zone during infiltration and the initial volumetric water content, as defined above.

For constant R_e, which is true if the crust is thin and unchanging, equation 11.53 can be integrated using the initial conditions of $I = 0$ at $t = 0$, to give

$$I^2 + 2K_s R_e \Delta\theta I = 2K_s \psi_f \Delta\theta t \tag{11.54}$$

Solving equation 11.54 using the quadratic formula gives a relation for cumulative-horizontal infiltration as

$$I = \Delta\theta \left[\left(K_u^2 R_e^2 + 2K_s \frac{\psi_f}{\Delta\theta} t \right)^{1/2} - K_s R_e \right] \tag{11.55}$$

It should be noted that, in the absence of a crust, equation 11.55 reduces to equation 11.10, and is valid for horizontal infiltration as well as for early periods of vertical infiltration. Because gravitational forces become important as the infiltration process continues in time, for vertical infiltration, equation 11.52 can be modified by adding the distance from the soil surface to the wetting front, or

$$\frac{dI}{dt} = \frac{K_s(\psi_f + L_f)}{K_s R_e + L_f} \tag{11.56}$$

which, from equation 11.5, can also be written as

$$\Delta\theta \frac{dL_f}{dt} = \frac{K_s(\psi_f + L_f)}{K_s R_e + L_f} \tag{11.57}$$

Integrating equation 11.57 with $L_f = 0$ at $t = 0$ gives

$$L_f - (\psi_f - K_s R_e) \ln \left(\frac{\psi_f + L_f}{\psi_f} \right) = \frac{K_s t}{\Delta\theta} \tag{11.58}$$

It should be noted that for large times, the second term on the left-hand side of equation 11.58 is very small compared to L_f. Therefore, L_f for the crusted case at large times can be written as

$$L_f = \frac{K_s t}{\Delta\theta} + \delta(t) \tag{11.59}$$

where $\delta(t)$ is a small-error term.

Substituting equation 11.59 into equation 11.58 yields L_f as a function of time

$$L_f = \frac{K_s t}{\Delta\theta} + (\psi_f - K_s R_e) \ln \left(\frac{\psi_f + \dfrac{K_u t}{\Delta\theta} + \delta(t)}{\psi_f} \right) \tag{11.60}$$

Neglecting $\delta(t)$ for very large times, the cumulative infiltration for vertical infiltration through a crusted soil surface can be expressed as

$$L_f = K_s t + \Delta\theta(\psi_f - K_s R_e) \ln \left(1 + \frac{K_u t}{\Delta\theta \psi_f} \right) \tag{11.61}$$

Figure 11.10 compares cumulative infiltration and infiltration rate for an uncrusted and crusted soil. For this example, the soil was assumed to have a saturated-hydraulic conductivity of 0.0004242 cm/min, a wetting-front effective suction of 47.99 cm, a value of $\Delta\theta$ of 0.4367, and a thin film of water (but no ponding) on the soil surface. For the crusted condition, a crust

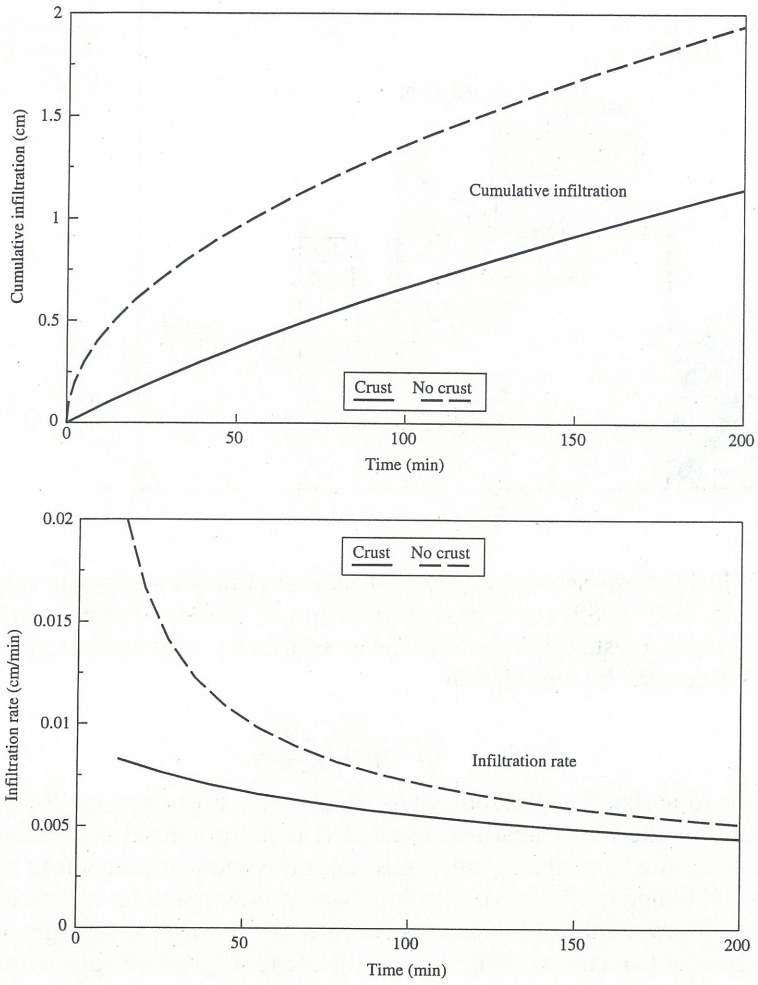

Figure 11.10 Green–Ampt cumulative infiltration and infiltration rates for crusted and uncrusted conditions

hydraulic resistance of 4,318 minutes and a thin crust was assumed. Equation 11.23 was solved for the uncrusted case by substituting $I/\Delta\theta$ for L_f. Using the same substitution, equation 11.58 was solved for the crust condition. Figure 11.10 indicates that the steady-state infiltration rate, given by equation 11.27, is approached sooner in crusted soil.

11.6 RUNOFF

The effects of infiltration rate on runoff quantity, duration, and distribution are well-known in hydrologic engineering. Often, runoff is estimated from strictly infiltration-based models; however, many runoff models take into account lumping of all losses—including infiltration, surface-depression storage, and interception of rainfall by vegetation growing on the surface. When rainfall (or other liquid inputs) begins on soil surfaces, a portion of the liquid is retained on vegetation or other surfaces, and is thus intercepted before it reaches the soil surface. Additionally, a portion of the liquid input may be retained at the soil surface in depressions, ranging in size from soil-grain-size cavities to ponds and lakes. A portion of the liquid is passed across the soil–atmosphere interface as infiltration, which is the most important liquid-input loss process under normal circumstances. Infiltration is a direct loss that governs the volume and rate of runoff, and highly influences the shape of the runoff hydrograph.

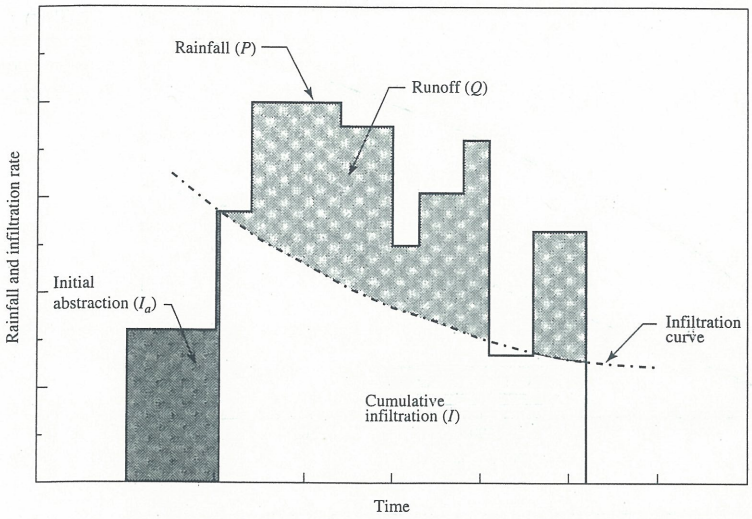

Figure 11.11 Schematic of the role of infiltration on runoff

Figure 11.11 shows schematically, the role that infiltration plays in runoff under storm conditions. The SCS (1980) combines infiltration with initial abstractions (interception and detention storage) to estimate the rainfall excess, which would appear as runoff. The runoff volume Q is estimated by the relation

$$Q = \frac{(P - I_a)^2}{P - I_a + S} \tag{11.62}$$

where Q is the total runoff expressed as a depth over the drainage area; P is the rainfall depth; I_a is the depth of the initial abstractions; and S is the potential maximum retention after runoff begins. As indicated above, initial abstractions include losses before runoff begins, and include water retained in surface depressions, water intercepted by vegetation and other surfaces, evaporation, and infiltration. Values of I_a are highly variable for a given drainage basin; however, SCS data from many small basins indicate that I_a can be approximated by

$$I_a = 0.2S. \tag{11.63}$$

If I_a from equation 11.63 is substituted into equation 11.62, then the SCS runoff relation becomes

$$Q = \frac{(P - 0.2S)^2}{P + 0.8S}. \tag{11.64}$$

Because S is related to the soil- and vegetative-cover properties of the drainage basin, it can be derived through the use of SCS runoff curve numbers CN (SCS 1980). Curve numbers have a range of between 30 and 100, and S is related to CN by

$$S = \frac{1000}{CN} - 10. \tag{11.65}$$

In addition to the above relation, the cumulative infiltration I also can be calculated from

$$I = P - I_a - Q. \tag{11.66}$$

It also can be noted that runoff does not occur until initial abstractions are satisfied. This leads to the two following relations which must be satisfied before runoff can occur

$$P \geq I_a \tag{11.67}$$

$$S \geq I_a + I \tag{11.68}$$

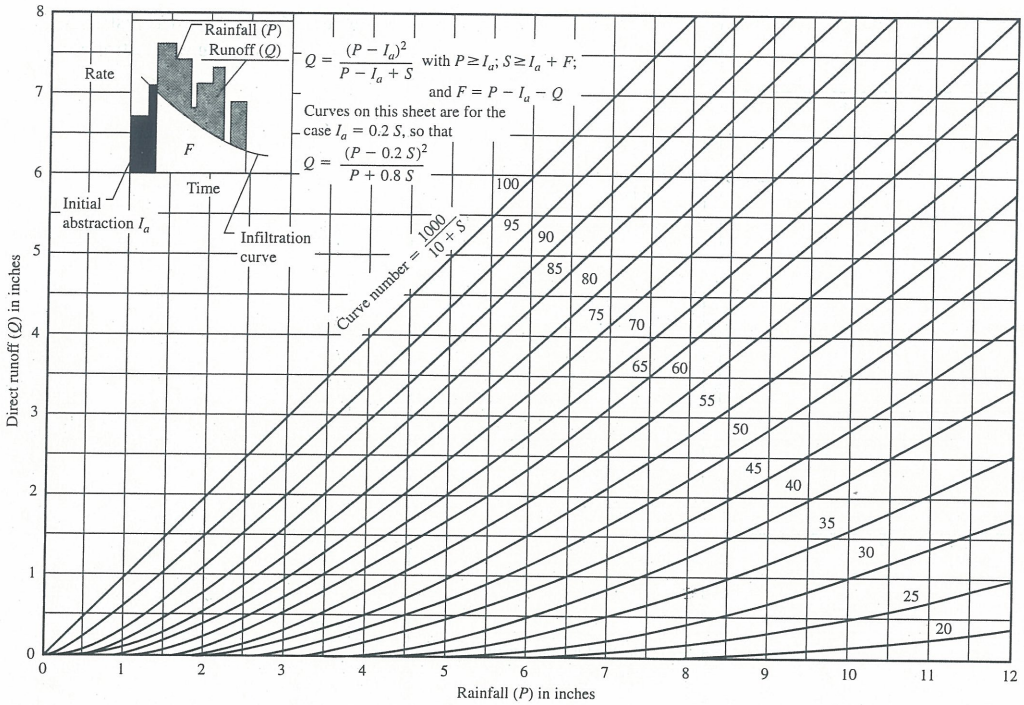

Figure 11.12 Graphical solution of equation 11.64

Figure 11.12 (SCS 1980) shows the relation between runoff and precipitation for various *CN*s, and is a solution to equation 11.64 for the particular case assumed by equation 11.63. Other definitions of the relation between I_a and S would result in slightly different solutions.

11.7 REDISTRIBUTION AND INTERNAL DRAINAGE

Moisture redistribution, as well as internal flux of infiltrated water, is highly dependent upon several factors described previously. These factors include the quantity of liquid reaching the soil surface and its distribution over time; the physical and chemical characteristics of the soil and the liquid; and other factors such as initial-moisture content, surface slope, vegetative cover, and surface roughness.

Water Redistribution

After an infiltration event, liquids infiltrating the soil surface are subject to redistribution downward by matric and gravity potentials, and removal across the soil–atmosphere interface by evapotranspiration. The quantity and rate of redistribution of infiltrated water in relation to the cumulative infiltration over time is discussed below, for a simple, rectangular water-redistribution profile (Charbeneau 1989), as discussed in chapter 13. Water redistribution is altered if the infiltration rate is less than the effective saturated-hydraulic conductivity, as opposed to an infiltration rate that is greater than the effective saturated-hydraulic conductivity (Bouwer 1966). These different infiltration rates also affect the water flux rates (internal drainage) within the soil profile.

Figure 11.13 shows the effects of infiltration on moisture redistribution in a sandy loam, whose properties have been defined by Rawls, Brakensiek, and Savabi (1982). Two cumulative infiltration values are shown, 4 cm in 4 hours (average infiltration rate i of 1.0 cm/hr) and

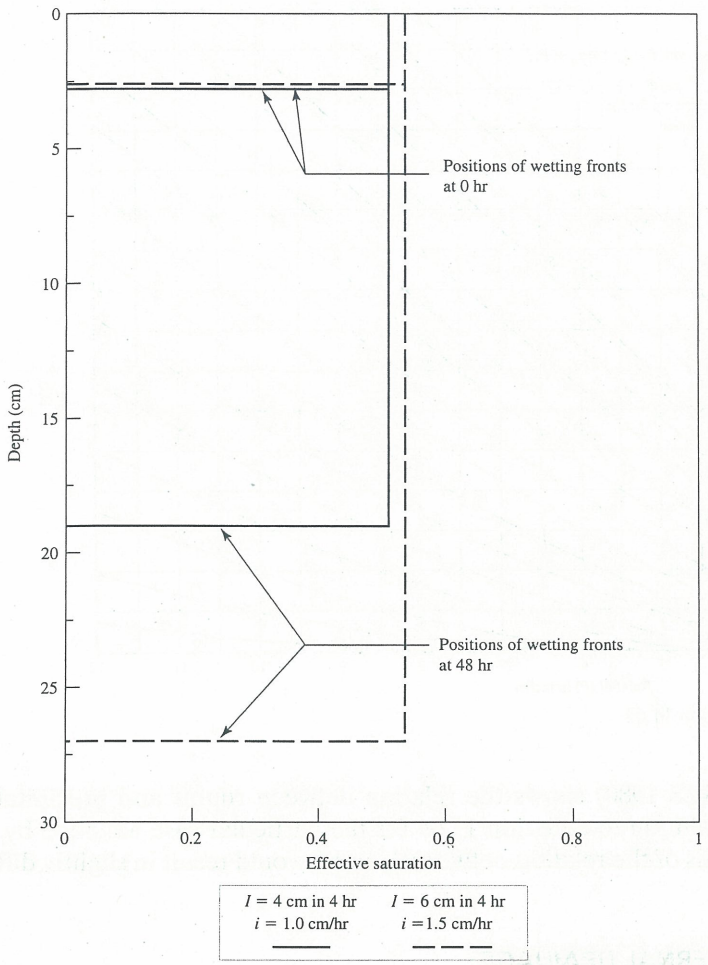

Figure 11.13 Water redistribution with changing infiltration rate

6 cm in 4 hours (i = 1.5 cm/hr). The simplified, rectangular water-redistribution profile, shown in figure 11.13, indicates that an average infiltration rate of 1 cm/hr (less than the effective saturated-hydraulic conductivity of 1.3 cm/hr) gives a wetting-front position of 19 cm below ground surface, with an effective saturation of 0.511 after 48 hours. However, an average infiltration rate of 1.5 cm/hr (greater than the effective saturated hydraulic conductivity) gives a wetting-front position of 27 cm below ground surface with an effective saturation of 0.537 after 48 hours. Both of these calculations assume that the initial soil-moisture content was at residual saturation. The difference in wetting-front movement is attributable to the increased moisture content and hydraulic conductivity from more infiltrated water. In general, a higher-average infiltration rate and/or a higher cumulative-infiltration results in wetting fronts that proceed deeper and faster into a soil column, with uniform properties, resulting in a higher degree of saturation.

Internal Drainage

Figure 11.14 shows the time-rate of change of Darcian flux, q, in the same sandy loam soil at a depth of 30 cm below ground surface, for the two cumulative infiltration values of 4 cm in 4 hours and 6 cm in 4 hours. For the average infiltration rate of 1.0 cm/hr, the wetting front arrives at a depth of 30 cm at a time of approximately 89.5 days, with an effective saturation

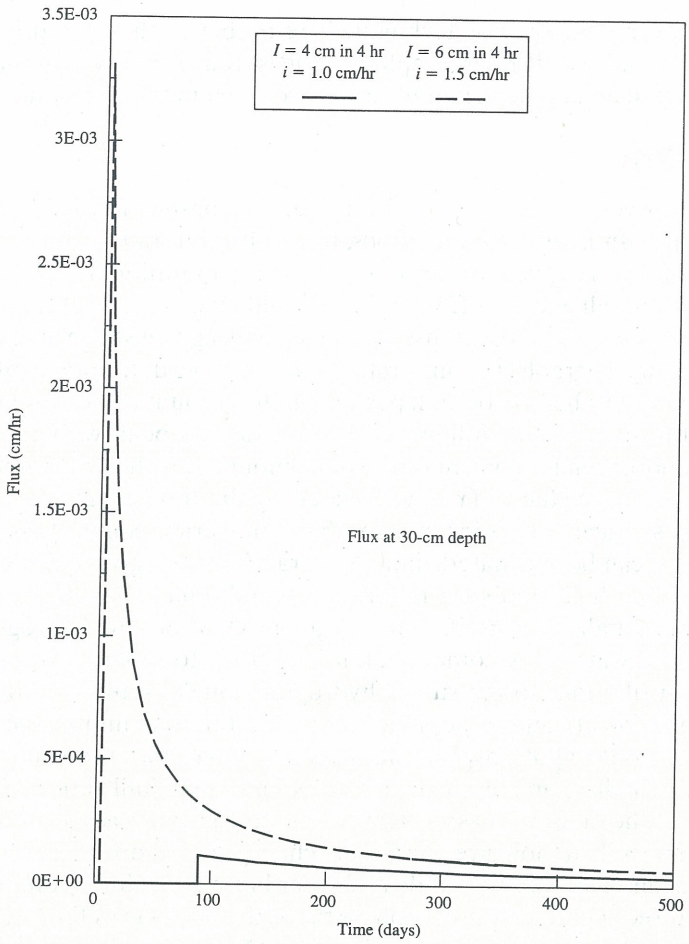

Figure 11.14 Change in water flux with changing infiltration rate

of 0.324. The wetting front for the higher infiltration rate of 1.5 cm/hr arrives at a depth of 30 cm at a time of approximately 4.6 days, with an effective saturation of 0.485. The peak flux rate for $i = 1.0$ cm/hr was calculated to be 1.2×10^{-4} cm/hr and the peak flux-rate for $i = 1.5$ cm/hr, was 3.3×10^{-3} cm/hr. The difference in these two wetting-front arrival times and peak flux rates is attributable to the additional increase in liquid from the higher-average infiltration rate. In general, a higher average-infiltration rate and/or a higher cumulative-infiltration results in substantially higher Darcian flux rates at a given depth in a soil column with uniform properties. The peak flux rates appear to change by orders of magnitude with less than a doubling of the cumulative infiltration.

11.8 FIELD MEASUREMENTS

Because infiltration is a complex process that varies both spatially and temporally, the selection of a measurement or data-analysis technique should consider the complexities involved. Infiltration-measurement techniques can be broadly categorized into two methods: **(1)** areal measurements (or data analysis); and **(2)** point measurements. Areal measurements and data analysis usually involve drainage basin or large-plot scales. Point measurements involve measurement of infiltration at a point in a small plot, using various techniques. It is generally felt that areal data-analysis techniques have the advantage over point measurements of infiltration because they relate more directly to prevailing conditions of precipitation and field

conditions. However, data-analysis techniques are no better than the precision with which both precipitation and runoff hydrographs are measured. Some typical measurement techniques for both areal and point-field infiltration are given in the following sections.

Areal Measurements or Data Analysis

Infiltration rate curves can be estimated for drainage basins and field plots by analyzing runoff hydrographs. In hydrograph methods, the infiltration rate is estimated by records of rainfall and runoff from a given drainage basin, with evaporation neglected. Theoretically, a detailed study of rainfall and runoff with time should give a reasonable estimate of infiltration rate. Because each period of intense rainfall during a given storm event produces a peak on the discharge hydrograph, the infiltration rate can be determined by subtracting the amount of runoff under the hydrograph peak from the amount of the rainfall. An example of this generalized technique is as follows: if the first rainfall peak with x cm of rainfall produced y cm of runoff, then $(x - y)$ cm is the total amount of water infiltrated during that part of the storm event. The value of $(x - y)$, divided by the time during which the rainfall occurred, gives the average infiltration rate for that time period. Similarly, infiltration rates for other time periods can be calculated, and an overall infiltration-rate curve can be obtained.

Hydrograph methods apply for relatively small drainage basins where there is a clear relation between rainfall and runoff. In drainage basins where the hydrograph is comprised of the large ground water flow component, it is difficult to separate the surface-water and ground water contributions to the runoff hydrograph, making the methods difficult to use. Other sources of difficulty and of possible errors in estimating infiltration rates, include the effects of evaporation/evapotranspiration, surface storage, and interception effects. In general, the validity of hydrograph methods for the estimation of infiltration rates is inversely related to the size of the drainage basin—because of the lag-times associated with the rainfall-runoff process, antecedent moisture conditions, changing meteorological conditions over the basin, and spatial and temporal variability of other basin hydrologic conditions.

There are three common hydrograph methods that use one of the following techniques: **(1)** detention-flow relations to derive rainfall excess; **(2)** time-condensation technique to eliminate periods of inadequate rainfall; and **(3)** block methods of dividing the rainfall into a series of blocks to obtain a succession of average infiltration rates over time. Each of these methods has been treated in detail by Musgrave and Holtan (1964), and are summarized below.

Detention-flow relation technique The essential features of this infiltration-rate estimation technique assume: **(1)** that the rain storm is of sufficient duration and intensity such that the infiltration rate will have become relatively constant; and **(2)** that the rainfall is intermittent so that the hydrograph rises and falls over the time-periods of interest; a single-peaked hydrograph would not provide enough information to determine an infiltration-rate curve. A step-by-step procedure for this method is available in Musgrave and Holtan (1964).

Time-condensation technique In this technique, variations in rainfall are eliminated by condensing time in order to obtain a constant rainfall rate, and then applying the same techniques used in analyzing rainfall simulator data. Time is condensed in a such a way as to cause the mass-rainfall curve to be a straight line over all time used in the analysis. Infiltration rate is estimated based on the assumptions that: **(1)** initial abstractions have been satisfied at the time runoff starts; **(2)** the curve of cumulative infiltration is parallel to the retention curve during periods of runoff; and **(3)** during periods of no runoff, the cumulative infiltration curve intersects the retention curve. Infiltration rate is then calculated as the slope of the cumulative infiltration-curve segments for various time periods. Musgrave and Holtan (1964) present more details on the use of this method.

Block technique The block technique is probably best-suited to estimating infiltration rates on larger drainage basins, because rainfall on larger basins is seldom known closely enough to warrant the use of either the detention-flow or time-condensation techniques. The

block, or average infiltration, technique involves preparing an isohyetal map for each storm. Each of the resulting storm hydrographs can be separated from the succeeding ones by transposing recession curves (Musgrave and Holtan 1964). The average infiltration rate is calculated for each storm event. Nachabe and others (1997) present methods for estimating infiltration over heterogeneous watersheds under the influence of spatially varying parameters, such as sorptivity and saturated-hydraulic conductivity.

Point Measurements

Point measurements of infiltration rate include specific types of infiltrometers whose results are applicable only at the locations and for the particular soil, vegetative, and other hydrologic conditions where the measurements are made. Point measurements have the advantage that rainfall/runoff data are not needed and that infiltration-rate tests can be repeated quickly, compared to areal analyses. Point-infiltration measurements fall into four categories: **(1)** rainfall simulators; **(2)** ring or cylinder infiltrometers; **(3)** tension infiltrometers; and **(4)** furrow methods (Rawls et al. 1993). Each of these infiltration-measurement techniques was specifically designed to mimic a given infiltration-process cause. For example, if the effect of raindrops is important at a given site, then rainfall simulators that use sprinkling are appropriate. If infiltration rates for flooded conditions are desired, then the ring or cylinder infiltrometer is used. Tension infiltrometers are used to measure infiltration rates on soil surfaces where macropores may be present. Furrow techniques are used where flowing water may affect infiltration rates.

Rainfall Simulators Simulation of rainfall using spray nozzles, drip screens, or drip towers has been used for infiltration and erosion measurements. The simulators attempt to reproduce the characteristics of natural rainfall, including raindrop-size distribution, raindrop velocity, as well as rainfall intensity and duration.

Spray nozzles, spaced at different intervals and at different heights above the soil surface, have been developed to produce raindrops of different sizes. The nozzles produce artificial rain when water is sprayed upward into the air and the drops are allowed to fall downward onto the surface of interest. Nozzles can be obtained commercially in a variety of types and sizes, for various water-pressure ranges.

Drip screens and drop towers have also been widely used to study the effects of rainfall on soil-surface erosion and to evaluate infiltration rates. The artificial raindrop size is controlled by the screen-mesh size and/or pieces of yarn of varying sizes, to obtain uniform raindrops. Raindrop velocity is controlled by varying the height of the apparatus, and intensity by varying the head of water used to produce the raindrops, or by reducing the size of the holes supplying water to the drip screen. Glass capillary tubes and hypodermic needles have been used to form simulated raindrops instead of pieces of yarn. Peterson and Bubenzer (1986) have inventoried and categorized rainfall simulators, and provide the details for constructing a rainfall simulator.

Ring or cylinder infiltrometers These infiltrometers are sometimes referred to as "flooding-type" infiltrometers. They are made of metal rings with diameters ranging from approximately 30 to 100 cm, and are 30 to 60 cm high. The metal rings are driven (jacked) into the soil to a depth of between 5 and 15 cm. The most common type of ring infiltrometer is the double-ring infiltrometer, which is a ring infiltrometer with a second, larger ring around it. Both rings have water applied to them, but measurements are only taken inside the inner ring; the outer ring serves as a buffer to help minimize lateral spreading and maintain vertical flow beneath the rings. The double-ring infiltrometer has been adopted by the American Society for Testing and Materials (ASTM 1994) as a standard test.

One of the major limitations of using ring infiltrometers is disturbance of the soil while the rings are being driven into place. The interface between the soil and the sides of the rings can be a preferred pathway for water and could result in abnormally high infiltration rates.

However, if the rings are left in place for a long period of time (say, several hours), the impact of this disturbance is reduced. A second problem associated with ring infiltrometers is entrapped air, which rises when a constant head of water is applied to the surface. This confined air in saturated soil impedes the downward movement of water. Ring infiltrometers usually produce higher steady-state infiltration rates compared to sprinkler infiltrometers (Rawls et al. 1993).

Generally, the larger the area used for infiltration, the more accurate the estimation of infiltration rate; to this end, infiltration basins have been proposed. These basins range in size from a few square meters to 1,000 m^2, and usually have border arrangements for impounding water. A given amount of water is applied to the basin and the rate of infiltration is recorded. It should be noted that small basins have limitations similar to those of ring infiltrometers, with entrapped air being the largest. In larger basins, the volume of water needed for infiltration is quite large, and the heads across the basin may be non-uniform due to varying topography.

Tension infiltrometers The tension, or disk, infiltrometer consists of a tension-control tube, a tube to measure change in water level, and a large disk with a porous membrane approximately the same diameter as the inner ring of a double-ring infiltrometer. These infiltrometers are commercially available and have been well tested (Watson and Luxmoore 1986; Ankeny, Kaspar, and Horton 1988; Perroux and White 1988). The advantage of a tension infiltrometer is that, by varying the tension on the device, certain pores in the media of interest can be eliminated from the flow process and the effects of pore size distribution can be determined. This is especially important where macropores are present.

Furrow techniques Infiltration-rate measurements for flowing water—and in particular furrow irrigation systems—can be made with either a blocked-furrow infiltrometer, recirculating-furrow infiltrometer, or an inflow/outflow measurement. The blocked-furrow technique consists of blocking off a section of up to 5 m of furrow, and then ponding water in the furrow. The water level in the furrow is kept at a constant depth by continually adding water until a constant infiltration rate (constant water addition) is achieved. The infiltration rate is calculated as the time-rate of water additions to the furrow.

The recirculating furrow technique involves a modification of the blocked furrow technique by continuously recycling water over the 5-m furrow segment. It is felt that this technique better simulates conditions of actual flowing water (Rawls et al. 1993).

In the inflow/outflow technique, infiltration rates along the furrow are calculated by taking the difference in measured flow rates, at both the upstream and downstream ends of the furrow segment, over time. In this case, the length of the furrow segment is more important, because this length determines the early-time infiltration rate. Flow rates are usually measured by flumes. The impact of water lost to storage in the soil needs to be considered during calculation of infiltration rates, as well.

Additional information on field-infiltration measurement techniques can be found in Klute (1986); this also contains many references and specific step-by-step procedures.

QUESTION 11.1

Using Darcy's equation for vertical flow:

$$q = -K\frac{dH}{dz} = -K\frac{d}{dz}(H_p - z)$$

where q is flux, H is total hydraulic head, H_p is pressure head, z is vertical distance from the soil surface downward, and K the hydraulic conductivity, and the Green–Ampt approximations develop the

relation of the form of $i = i_c + b/I$ that expresses the infiltration rate as a function of the parameters given in the following figure.

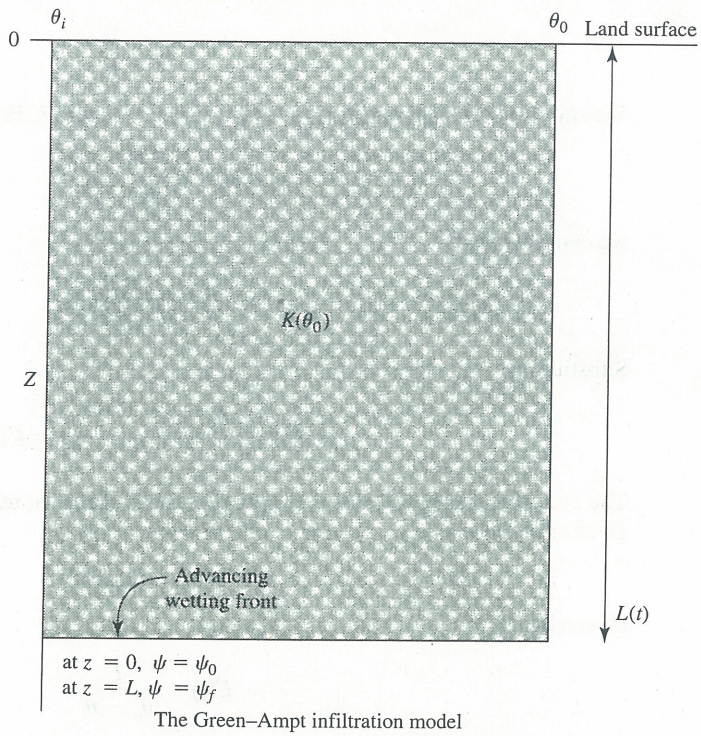

The Green–Ampt infiltration model

QUESTION 11.2

Considering question 11.1, what happens to the infiltration rate when t is small? What happens to the infiltration rate when t is large?

QUESTION 11.3

Given:

$$K(\theta_o) = 0.001 \text{ cm/s} = 3.6 \text{ cm/hr}$$
$$\Delta h = h_o - h_f = 40 \text{ cm}$$
$$\Delta\theta = \theta_o - \theta_i = 0.35$$

Calculate and plot cumulative infiltration I versus time and plot infiltration rate ($\Delta I/\Delta t$), I versus time for the first three hours of infiltration, for both the horizontal and vertical case.

SUMMARY

In this chapter, we presented the topics of infiltration; profile-water distribution; soil characteristics that affect infiltration; several of the most common infiltration models; and a comparison of various physically based infiltration models. We discussed the effects macroporosity, layered soils, and crusted soils each have on infiltration. Additionally, we examined the effects of infiltration rate on runoff quantity, duration, and distribution, redistribution and internal drainage, and various methods used for field measurement of infiltration.

ANSWERS TO QUESTIONS*

11.1. The general form of the Green–Ampt equation is

$$i = i_c + \frac{b}{I}$$

We want to derive an expression for I in terms of i_c and b. From

$$q = K\frac{d\psi}{dz} + K$$

we can state that

$$i = q = K\frac{d\psi}{dz} + K$$

Substituting

$$i = K(\theta_o)\left(\frac{\psi_f - \psi_o}{L}(t) - 0\right) + K(\theta_o) \tag{11.69}$$

The cumulative infiltration I is simply the total volume of water that has entered the profile at a given time t:

$$I = (\theta_o - \theta_i)\, L(t)$$

Rearranging:

$$L(t) = \frac{I}{\theta_o - \theta_i}$$

Substituting into equation 11.69, we have

$$i = K(\theta_o)\frac{\Delta\psi\,\Delta\theta}{I} + K(\theta_o) \tag{11.70}$$

where $\Delta\psi = \psi_f - \psi_o$ and $\Delta\theta = \theta_o - \theta_i$. Therefore, $i_c = K(\theta_o)$ and $b = K(\theta_o)\,\Delta\psi\,\Delta\theta$.

11.2. From equation 11.70, we can see mathematically that when t is small, the infiltration rate is very large. However, as t increases, the infiltration rate will asymptotically approach $K(\theta_o)$.

11.3. Using the Green–Ampt model, the following relations can be derived:

For one-dimensional horizontal infiltration,

$$I = \Delta\theta\,(2D_o t)^{1/2}$$

where

$$D_o = K(\theta_o)\frac{\Delta h}{\Delta\theta}$$

For one-dimensional vertical infiltration,

$$t = (1 - \xi)\ln\left(1 + \frac{1}{\xi}\right)\frac{1}{K(\theta_o)}$$

where

$$\xi = \Delta h\,\Delta\theta$$

*Questions 11.1–3 and the figure for question 11.1 were extracted from the unsaturated zone hydrology course taught at the United States Geological Survey's National Training Center in Denver, Colorado.

and

$$\Delta h = h_o - h_f > 0, \quad \Delta\theta = \theta_o - \theta_i > 0$$

Note that the equation for the vertical case is implicit.

Using these relations, we can tabulate the data, shown below. We leave it to the student to perform the actual plot of the data obtained.

One-Dimensional Horizontal			One-Dimensional Vertical		
I cm^3	time (hours)	i cm^3/hr	I cm^3	time (hours)	i cm^3/hr
0.000000	0.00	44.90	0.000000	0.00	55.15
2.244994	0.05	14.97	2.000000	0.04	23.80
4.489989	0.20	10.09	3.000000	0.08	18.02
5.499091	0.30	8.51	4.000000	0.13	13.72
6.349803	0.40	7.14	6.000000	0.28	10.82
7.776889	0.60	6.02	8.000000	0.46	9.21
8.979978	0.80	5.30	10.000000	0.68	8.19
10.039920	1.00	4.79	12.000000	0.93	7.48
10.998182	1.20	4.41	14.000000	1.19	6.96
11.879394	1.40	4.10	16.000000	1.48	6.57
12.699606	1.60	3.85	18.000000	1.79	6.25
13.469967	1.80	3.64	20.000000	2.10	6.00
14.198591	2.00	3.47	22.000000	2.44	5.79
14.891608	2.20	3.31	24.000000	2.78	5.62
15.553778	2.40	3.18	26.000000	3.14	5.47
16.188885	2.60	3.06	28.000000	3.51	5.34
16.800000	2.80	2.95	30.000000	3.88	5.05
17.389652	3.00		40.000000	5.86	

From the plots of I and i versus time, we see that at early times (< 2 hours), the amount of infiltrated water and the infiltration rate are very similar for horizontal and vertical infiltration. This is because the dominant driving force is the suction gradient and the driving force due to gravity is relatively small. However, as time increases, the suction gradient decreases, hence the relative magnitude of the effect of gravity increases. Therefore, vertical infiltration occurs at a rate that is greater than horizontal infiltration. At very large times, the suction gradient diminishes. In the case of horizontal infiltration, this results in a continually decreasing infiltration. In the case of vertical infiltration, it results in an infiltration rate that asymptotically approaches the saturated-hydraulic conductivity. This means that for early times, the shape of the wetting front for three-dimensional infiltration will be spherical. As time progresses, the horizontal movement of the wetting front will slow down relative to the vertical movement, and eventually most flow will be in the vertical direction.

ADDITIONAL QUESTIONS

11.4. A Laveen loam has the following infiltration hydraulic properties: $\Delta\psi = 25$ cm, $K_s = 0.45$ cm/hr, $\theta_t = 0.38$, and $\theta_i = 0.30$. Find the vertical infiltration rates and plot them versus time, for the Green–Ampt, Philip, Morel-Seytoux and Khanji, and Smith and Parlange models. Assume a value of $\beta = 1.35$ for the Morel-Seytoux and Khanji model, and that there is a thin film of water on the soil surface.

11.5. A water district disposes of reclaimed wastewater by sprinkler irrigating a large area of fallow land. The application rate is spatially uniform and constant at -3.0×10^4 cm^3 sec^{-1} cm^{-2} and has been continuous for some time, such that steady-state conditions exist in the subsurface. The negative sign indicates that the flux is downward. The soil beneath the site is layered, as sketched in

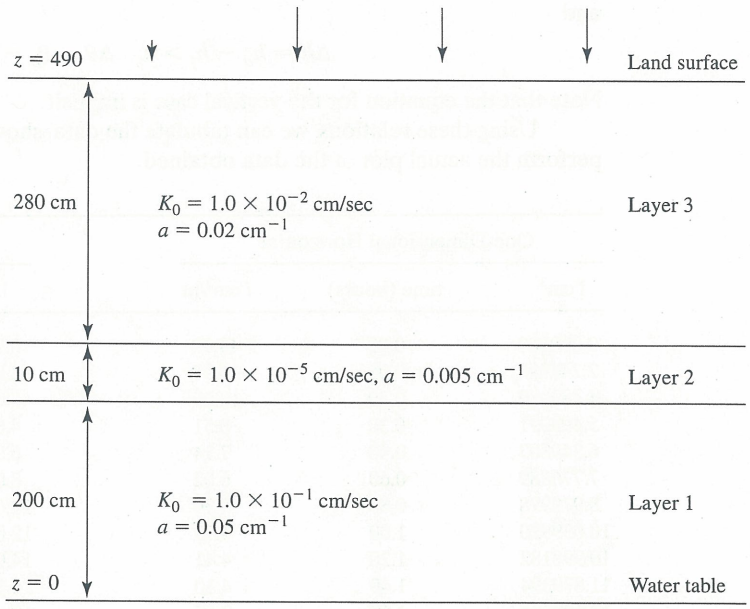

the accompanying figure. The $K(\psi)$ relation for each layer is $K(\psi) = K_o e^{-a\psi}$ and the parameters for each layer are given in the sketch below. The water table is located 4.9 m below the surface. Determine and plot the profiles of matric suction head $\psi(z)$ and the hydraulic head $H(z)$, between the water table $z = 0$ cm, and the ground surface $z = 490$ cm. Indicate saturated and unsaturated regions as appropriate. Explain the features of the profiles such as sign changes, magnitude of gradients, and so on.